Ceramics International 49 (2023) 7099–7104

Contents lists available at ScienceDirect

Ceramics International

journal homepage: www.elsevier.com/locate/ceramint

Short communication

$NaNbO_3$/Eumelanin composite: A new photocatalyst under visible light

Daiane Fernandes [a,*], Cristiane W. Raubach [a], Mateus M. Ferrer [a], Pedro L.G. Jardim [a,b], Carlos Frederico de O. Graeff [c,d], Mario L. Moreira [a,b], Eduardo C. Moreira [e], Valmor R. Mastelaro [f], Sergio da S. Cava [a,b]

[a] Post-Graduate Program in Materials Science and Engineering, Federal University of Pelotas, 96010-610, Pelotas, RS, Brazil
[b] Post-Graduate Program in Physics, Federal University of Pelotas, 96160-000, Capão do Leão, RS, Brazil
[c] Post-Graduate Program in Materials Science and Technology, São Paulo State University, 17033-360, Bauru, SP, Brazil
[d] Department of Physics, São Paulo State University, 17033-360, Bauru, SP, Brazil
[e] Spectroscopy Laboratory, Federal University of Pampa, 96413-172, Bagé, RS, Brazil
[f] Physics Institute, São Paulo University, 13560-970, São Carlos, SP, Brazil

ARTICLE INFO

Keywords:
Sodium niobate
Eumelanin
Photocatalysis
Visible light

ABSTRACT

Sodium niobate ($NaNbO_3$) is a semiconductor with many potential technological applications and, among them, it is considered a promising photocatalyst. However, it only absorbs ultraviolet light, limiting its use in light-dependent processes. Therefore, in this work we synthesized $NaNbO_3$ nanoparticles quickly and used them to prepare a $NaNbO_3$/Eumelanin composite with photocatalytic activity under visible light. Eumelanin was extracted from human hair and is a pigment responsible for the brown-black coloration, abundant in fauna and flora. The results showed that the composite successfully degraded the Rhodamine B dye. Therefore, this study presents a photocatalyst solution with better use of light and serves as inspiration for the development of new photocatalysts.

1. Introduction

Sodium niobate ($NaNbO_3$) is a semiconductor with many potential technological applications and, among them, photocatalysis [1–13]. It is considered a promising photocatalyst since it is thermodynamically stable, corrosion resistant and non-toxic [3,7]. However, the natural shape of its particle is cubic with low with low photocatalytic activity, but researchers have demonstrated that it is possible to obtain nanowires with high photocatalytic activity [5,12,13]. Another shape particle in nanoscale was presented by Farooq et al. [11] through the method polymeric citrate precursors for 22 h and calcination for 12 h, with high photocatalytic activity. In addition, it only absorbs ultraviolet light, limiting its use. Thus, to make the most of solar radiation, also promoting efficiency in the separation of photoinduced charges, $NaNbO_3$ was combined with other materials, forming heterostructured photocatalysts. The literature has shown great advances in photocatalytic processes using the strategy of building heterostructures [14–18]. Materials such as Cu_2O, Cu, Au, BiOI, Ag_2O, Ag_2SO_3, and Bi_2WO_6 were combined with $NaNbO_3$ for this purpose [19–25]. Nevertheless, the use of these metals ends up not being economically favorable.

Eumelanin is a pigment present in abundance in fauna and flora, responsible for the black-brown color. It is composed of disordered heteroaromatic networks based on 5,6-dihydroxyindole (DHI) and 5,6-dihydroxyindole carboxylic acid (DHICA) building blocks, which are catechol-derivatives [26–28]. It has many physicochemical properties, of particular interest here is a wide optical absorption ranging from UV to near-infrared (NIR), redox activity and metal-chelating capability [28–30]. Eumelanin and a similar polymer polydopamine (PDA) have been considered in different application [31–38]. In photocatalytic applications, composites with TiO_2, Cds, CuO_2, BiOBr, and MIL-53(Fe) were reported [28,39–50].

Considering the above, we present a rapid method to synthesize NaNbO3 nanoparticles similar to nanograins. These nanoparticles were used to prepare for the first time a NaNbO3/Eumelanin composite with photocatalytic activity under visible light. The photocatalytic activity was analyzed through the degradation of Rhodamine B (RhB), a dye widely used in industry and highly toxic [51].

* Corresponding author.
E-mail address: daiane.fg.eng@outlook.com (D. Fernandes).

https://doi.org/10.1016/j.ceramint.2022.12.094
Received 25 July 2022; Received in revised form 25 November 2022; Accepted 12 December 2022
Available online 14 December 2022

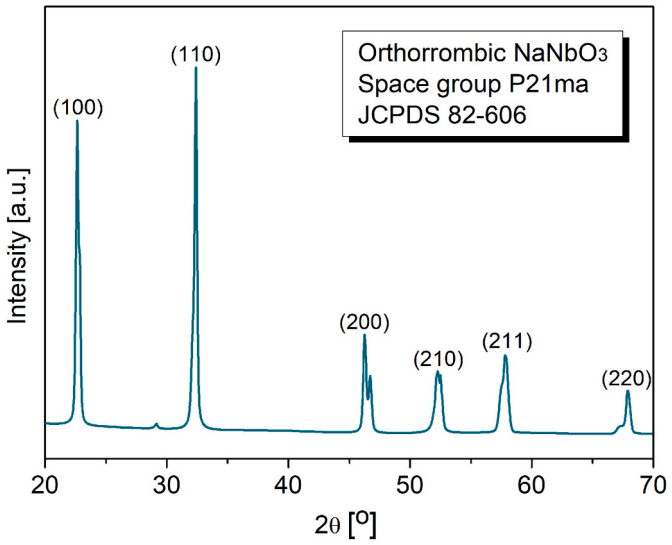

Fig. 1a. XRD of the $NaNbO_3$.

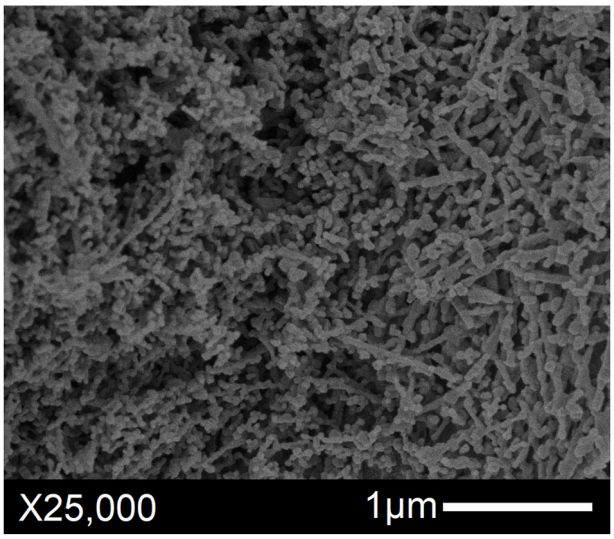

Fig. 1b. SEM of the $NaNbO_3$.

2. Experimental

2.1. $NaNbO_3$ synthesis

An aqueous solution of NaOH (Merck, 99.0%) and NbCl5 (CBMM, 99.0%) with concentrations of 6 M and 0.6 M, respectively, was taken to an adapted microwave oven (800 W, PANASONIC) for 15 min at 180 °C. The obtained precipitate was washed and centrifuged until the pH was neutralized and then dried in an oven. Finally, the powder was submitted to thermal treatment at 800 °C for 2 h and naturally cooled.

2.2. Eumelanin extraction

Eumelanin was extracted from dark brown human hair using the acid isolation method [33]. 2 g of clean hair was immersed in HCl (37%, 70 mL) at 100 °C for 3 h. Finally, the Eumelanin was collected by centrifugation and washed until solution had a neutral pH and then dried in an oven.

2.3. Preparation of $NaNbO_3$/Eumelanin composite

The composite was prepared according to the method reported by Xie. et al. [35]. A solution of 50 ml of ethanol, 4 mg of Eumelanin and 16 mg of NaNbO3 was sonicated for 30 min and stirred for 5 h at room temperature. The homogeneous suspension was dried in an oven.

2.4. Sample characterization

X-ray diffraction was performed in a diffractometer (Ultima IV, RIGAKU) with Cu-Kα radiation (λ = 1.5406 Å), scanning of 10°/min. Raman spectroscopy were done using a micro-positioning system (B&WTek, RAMAN PROBE) and monochromator (Shamrock 303i, ANDOR) with 532 nm excitation. High resolution images were taken using Scanning Electron Microscope, (JSM7500F, JEOL). Optical absorption spectra were obtained using a UV–Vis–NIR spectrometer (Lambda 1050, PERKIN ELMER). The valence band top potential was estimated by X-ray photoelectron spectroscopy (XPS) using a spectrometer (ESCA+, SCIENTIA OMICRON) with a high performance hemispherical analyzer (EAC2000) and monochromatic Al-Kα radiation (hν = 1486.6 eV). In addition, we evaluated the photoluminescence and textural properties of samples (supplementary data file).

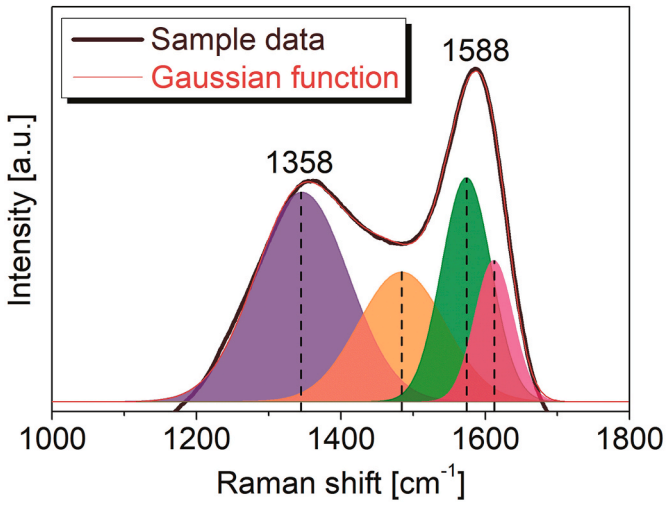

Fig. 2a. Raman spectra of the Eumelanin.

2.5. Photocatalytic activity

The photocatalytic activity was evaluated under visible irradiation, using a 100 W LED (MEGAACE, 400 nm < λ < 800 nm, int. máx at 458 and 538 nm). The photocatalytic reaction was carried out with 10 mg of the photocatalyst dispersed in 50 mL of RhB solution (5 mg.L-1), under magnetic stirring at room temperature, which was first stirred for 1 h in the dark. The variation in RhB concentration was recorded by absorbance, using a UV–Vis spectrophotometer (SP200 UV, BEL PHOTONICS).

3. Results and discussion

Fig. 1a show the XRD of NaNbO3 sample. The peaks shown in the diffractogram are characteristic of the orthorhombic phase, space group P21ma (JCPDS card files, 82–606). In addition, the mean value of the crystallographic domains was estimated by the Scherrer equation, resulting 27.43 nm. The NaNbO3 obtained presents particle shape similar to nanograins, with an average size of ~28 nm (Fig. 1b).

Fig. 2a shows the Raman spectrum of the extracted Eumelanin. It is possible to observe two bands around 1358 and 1588 cm−1, which are characteristic of disordered graphitic materials, the D and G bands, [35,

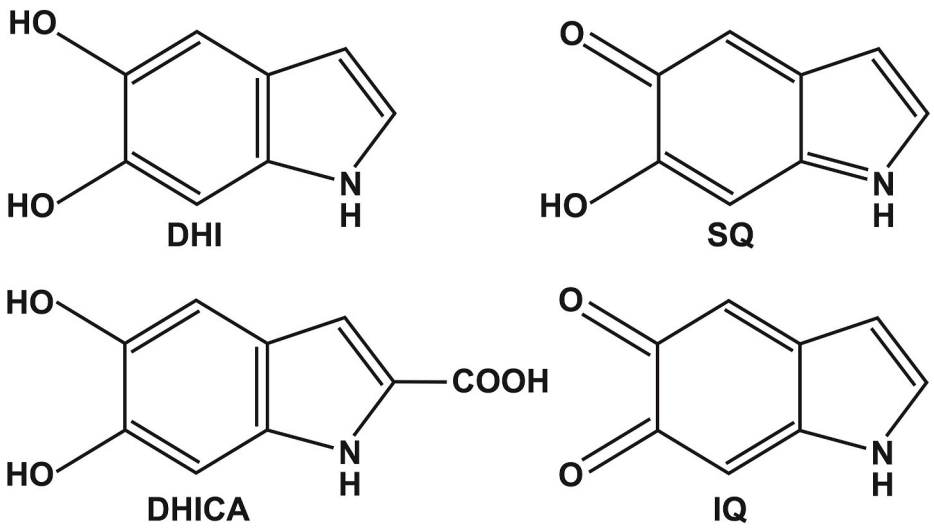

Fig. 2b. DHI, DHICA, SQ and IQ structures.

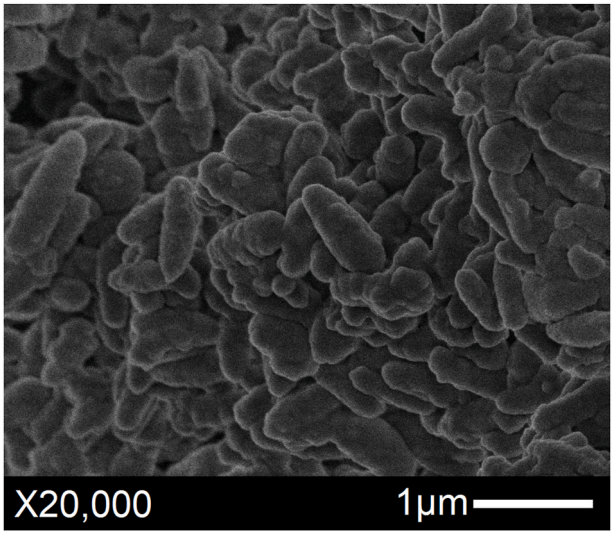

Fig. 2c. SEM of the Eumelanin.

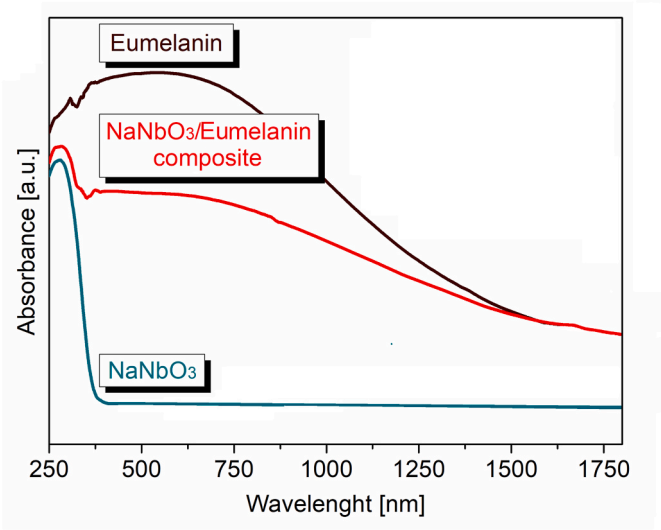

Fig. 3a. Optical absorbance spectra of the samples.

52]. Studies indicate that melanin has a graphene sheet-like structure with high-density of vacancy defects [52]. Through deconvolution, using the Gaussian function, four vibrational modes are also observed assigned to their functional groups. The band at ~1344 cm−1 corresponds to the C–OH phenolic stretching (DHI/DHICA) and C–O stretching of the carboxylic acid, the band at ~1484 cm−1 is attributed to the C–N group in the IQ, band at ~1574 cm-1 is attributed to the C═N stretching (in SQ) or the N–H bending vibration (in IQ) and the band at ~1600 cm−1 corresponds to aromatic C═C bond in the indole structure [35,53]. Fig. 2b shows the basic units of Eumelanin DHI and DHICA and their redox forms (5,6-indolequinone (IQ) and semiquinone (SQ)) [35, 53]. The extracted Eumelanin presents ellipsoidal shaped particles, with principal axis of ~400 nm and ~1 μm (Fig. 2c), in good agreement with literature [35,54,55].

Fig. 3a shows the optical absorbance spectra of the samples. NaNbO3 shows intense absorption in the UV region only and Eumelanin has a broadband absorption spectrum, due to the overlap of a range of absorption peaks of the DHI and DHICA oligomers [56,57]. In Eumelanin, the electronic states do not have a definite low-energy edge for optical absorption, but tail states [30,56]. Its band gap is associated with the transitions π-π* between molecular orbitals in HOMO (highest occupied molecular orbital) and LUMO (lowest unoccupied molecular orbital) [39,45,56]. The composite maintains the broadband absorption of Eumelanin (Fig. 3a), a little reduced due to NaNbO3 nanoparticles that decorate its surface (Fig. 3b), by Van der Waals interactions, which is possible due to its strong affinity for metallic cations.

The photocatalytic activity of the samples was evaluated through the photo-induced degradation of RhB, where C0 and C indicate the initial concentration and concentration at a specific time (h), respectively (Fig. 3c). It is observed that only the NaNbO3/Eumelanin composite showed photocatalytic activity, inducing ~96% of dye degradation in 5 h. Although Eumelanin presents high absorption in the visible range, its photocatalytic activity is unsatisfactory. This is because the π-system allows for high mobility of charge carriers, wich can easily recombine. To better understand the dye degradation mechanism, experiments to identify the active species were performed. For this, isopropyl alcohol (C3H8O), silver nitrate (AgNO3), and disodium ethylenediaminetetraacetate (EDTA) were used as scavengers for hydroxyl radicals (·OH), electrons (e−), and holes (h+), respectively. Fig. 3d shows the percentual of RhB degradation with the presence of scavengers at the end of 5 h. It is observed that the addition of EDTA and C3H8O inhibited the degradation of the dye, indicating that the main active species during the photocatalysis process are h+ and ·OH. In contrast, the addition of AgNO3 no change in the percentual, indicating that the e−are not active

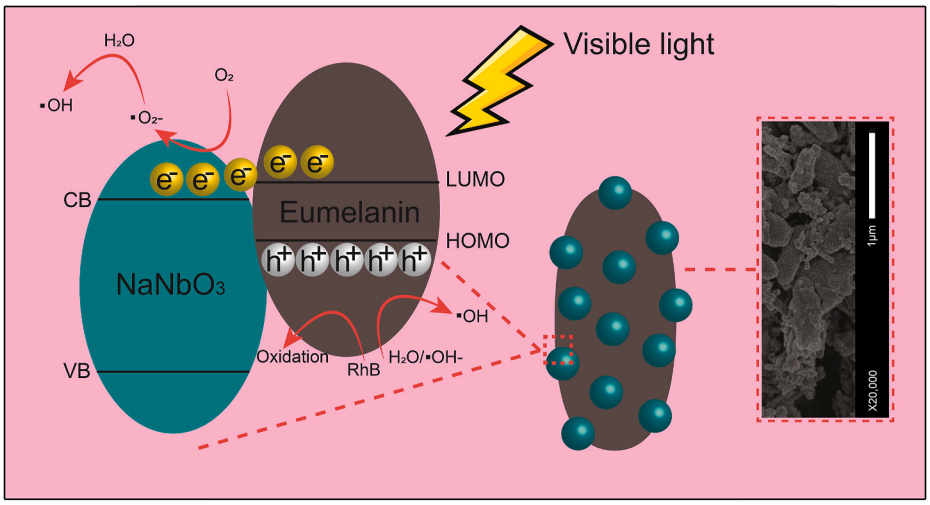

Fig. 3b. Schematic illustration of the possible mechanism for photodegradation of the RhB, under visible light and SEM-FEG of the $NaNbO_3$/Eumelanin composite.

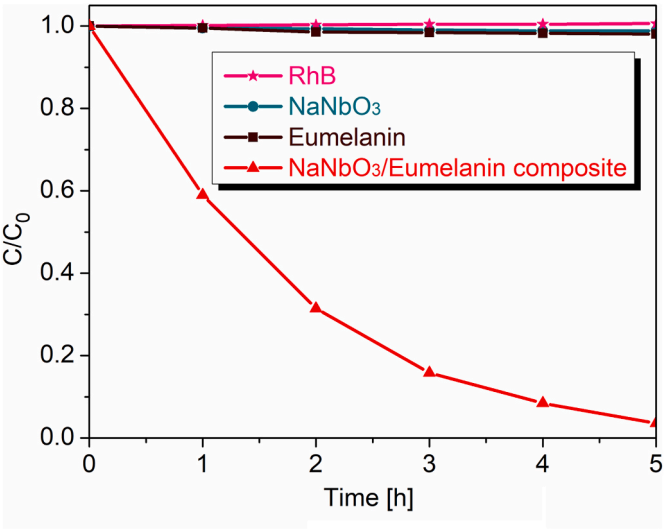

Fig. 3c. Photocatalytic degradation of the RhB under visible light irradiation.

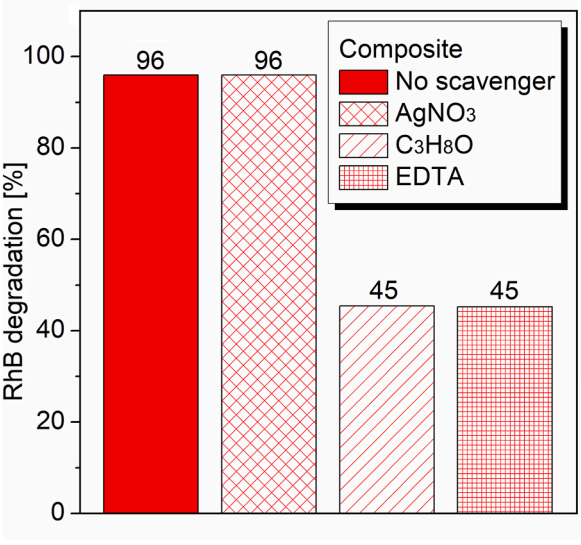

Fig. 3d. Percentage of RhB degradation using scavengers.

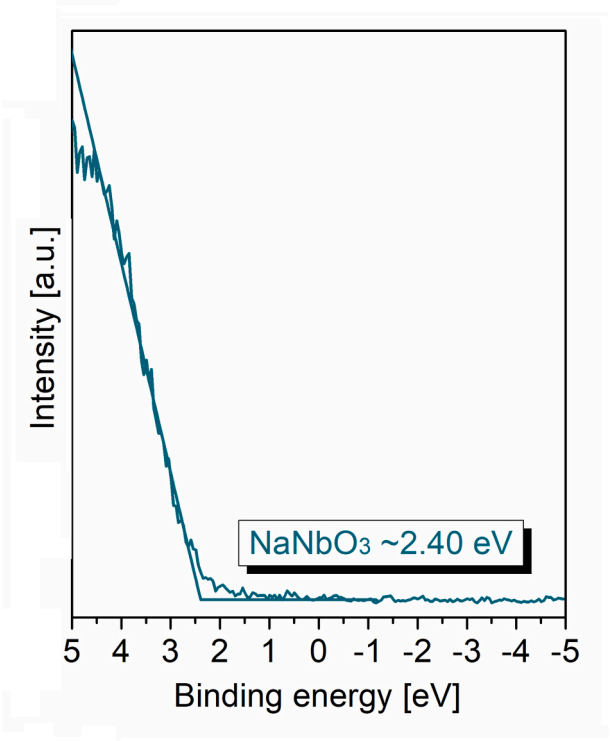

Fig. 4a. Valence-band XPS spectra of the $NaNbO_3$.

species. In addition, a reuse test was carried out. After three successive cycles, the composite maintained the same photocatalytic efficiency, demonstrating that it can be considered a stable photocatalyst.

Based on the results, a possible mechanism is proposed (Fig. 3b). Under visible light irradiation, only the electrons of Eumelanin are excited, from HOMO to LUMO, forming an electron/hole pair (e−/h+). The electrons in LUMO are injected into the CB, due to the potential difference. The electrons in the CB can react with oxygen (O2) to produce superoxide radical (•O2-), that can react with water (H2O) to produce •OH. Meanwhile, h+ in LUMO can react with H2O or hydroxyl anion (•OH-) to generate •OH and also directly oxidize the RhB dye. With this, an efficient separation of charge and a slower recombination are achieved, resulting in a significant increase in photocatalytic activity. This agrees with the results obtained in the experiment of active

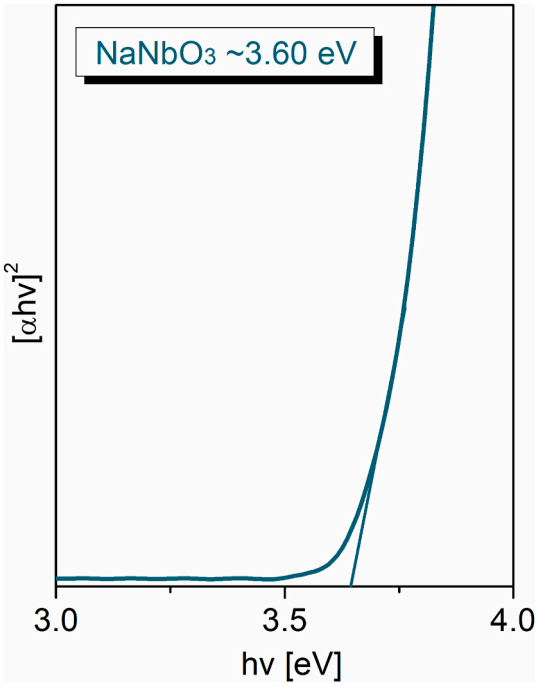

Fig. 4b. Band gap of the $NaNbO_3$.

species (Fig. 3d) and also with the photoluminescence analysis (Fig. S1).

Potentials of edge of NaNbO3 were determined by the equation Ecb = Evb – Eg, where Ecb is potential of the bottom of the CB, Evb is the potential at the top of the VB and Eg is the band gap energy. According to XPS, Evb is +2.40 eV (Fig. 4a). The band gap was estimated in 3.60 eV (Fig. 4b), by the Wood/Tauc method [58], resulting in −1.20 eV the Ecb. The direct location of the HOMO and LUMO of the natural Eumelanin is very difficult to determine due to its structural and energetic disorder. Because of this, researches asume that it is close to that of PDA [59]. The LUMO of the PDA is estimated at −1.4 eV [42,48,60]. Thus, the LUMO of Eumelanin is more electronegative than the CB of NaNbO3 making it possible to transfer charges in the NaNbO3/Eumelanin composite, as proposed in Fig. 3b.

4. Conclusions

In this work, NaNbO3 nanograins were obtained by microwave-assisted hydrothermal method followed by heat treatment. The nanoparticles were used to prepare a NaNbO3/Eumelanin composite with photocatalytic activity under visible light. The results showed that pure NaNbO3 and pure Eumelanin do not show photocatalytic activity, while the composite was able to successfully degrade the RhB dye. The heterostructure promoted efficient separation of photogenerated charges and slower recombination, resulting in a significant increase in photocatalytic activity. Therefore, this study presents an alternative photocatalyst that uses visible light and widely available elements, serving as inspiration for the development of new photocatalysts.

Declaration of competing interest

The authors declare that they have no known competing financial interests or personal relationships that could have appeared to influence the work reported in this paper.

Acknowledgments

The authors thank Companhia Brasileira de Metalurgia e Mineração (CBMM) for donating the niobium precursor, Núcleo de Apoio à Pesquisa em Ciência e Engenharia de Materiais (NAPCEM-UNIFESP Campus São José dos Campos) for XRD analysis, Centro Integrado de Análises (CIA FURG) for BET analysis and to colleagues Paola Gay, Thissiana Fernandes, Lucas Affonço, Ramon Dadalto, Caroline Schmechel and Lucas Barcellos for supporting. This research received support from Coordenação de Aperfeiçoamento de Pessoal de Nível Superior (CAPES), Conselho Nacional de Desenvolvimento Científico e Tecnológico (CNPq) and Fundação de Amparo à Pesquisa do Estado do Rio Grande do Sul (FAPERGS) (17/25510000889-8).

Appendix A. Supplementary data

Supplementary data to this article can be found online at https://doi.org/10.1016/j.ceramint.2022.12.094.

References

[1] D. Fernandes, M.M. Ferrer, C.W. Raubach, M.L. Moreira, P.L.G. Jardim, E. C. Moreira, C.F.O. Graeff, S.S. Cava, Fast synthesis of NaNbO3 nanoparticles with high photocatalytic activity for degradation of organic dyes, J. Am. Ceram. Soc. 106 (2022) 399–409, https://doi.org/10.1111/jace.18740.

[2] H. Shi, T. Wang, J. Chen, C. Zhu, J. Ye, Z. Zou, Photoreduction of carbon dioxide over NaNbO3 nanostructured photocatalysts, Catal. Lett. 141 (2011) 525–530, https://doi.org/10.1007/s10562-010-0482-1.

[3] P. Li, S. Ouyang, G. Xi, T. Kako, J. Ye, The effects of crystal structure and electronic structure on photocatalytic H2 evolution and CO2 reduction over two phases of perovskite-structured NaNbO3, J. Phys. Chem. C 116 (2012) 7621–7628, https://doi.org/10.1021/jp210106b.

[4] G. Li, Z. Yi, Y. Bai, W. Zhang, H. Zhang, Anisotropy in photocatalytic oxidization activity of NaNbO3 photocatalyst, Dalton Trans. 41 (2012), 10194, https://doi.org/10.1039/c2dt30593c.

[5] Q. Liu, L. Zhang, Y. Chai, W.-L. Dai, Facile fabrication and mechanism of single-crystal sodium niobate photocatalyst: insight into the structure features influence on photocatalytic performance for H2 evolution, J. Phys. Chem. C 121 (2017) 25898–25907, https://doi.org/10.1021/acs.jpcc.7b08819.

[6] F. Fresno, P. Jana, P. Reñones, J.M. Coronado, D.P. Serrano, V.A. O'shea, CO2 reduction over NaNbO3 and NaTaO3 perovskite photocatalysts, Photochem. Photobiol. Sci. 16 (2017) 17–23, https://doi.org/10.1039/C6PP00235H.

[7] T. Ahmad, U. Farooq, R. Phul, Fabrication and photocatalytic applications of perovskite materials with special emphasis on alkali metal based niobates and tantalates, Ind. Eng. Chem. Res. 52 (2018), https://doi.org/10.1021/acs.iecr.7b04641, 18–4.

[8] M. Nawaz, S.A. Almofty, F. Qureshi, Preparation, formation mechanism, photocatalytic, cytotoxicity and antioxidant activity of sodium niobate nanocubes, PLoS One 13 (2018), e0204061, https://doi.org/10.1371/journal.pone.0204061.

[9] N. Duc Van, Template-free synthesis and photocatalytic activity of {001}-facets exposed rhombohedral NaNbO3 microcrystals, Ceram. Int. 44 (2018) 19945–19949, https://doi.org/10.1016/j.ceramint.2018.07.260.

[10] A. Hamilton, S. O'donnell, B. Zoellner, I. Sullivan, P. Maggard, Flux-mediated synthesis and photocatalytic activity of NaNbO3 particles, J. Am. Ceram. Soc. 103 (2019) 454–464, https://doi.org/10.1111/jace.16765.

[11] U. Farooq, R. Phul, S. Alshehri, J. Ahmed, T. Ahmad, Electrocatalytic and enhanced photocatalytic applications of sodium niobate nanoparticles developed by citrate precursor route, Sci. Rep. 9 (2019) 4488, https://doi.org/10.1038/s41598-019-40745-w.

[12] C. Yan, B. Li, J. Wang, A comparative study of photodegradation behavior sodium niobate nanowires and microcubes, Key Eng. Mater. 861 (2020) 221–227. https://doi.org/10.4028/www.scientific.net/KEM.861.221.

[13] D. Fernandes, C.W. Raubach, P.L.G. Jardim, M.L. Moreira, S.S. Cava, Synthesis of NaNbO3 nanowires and their photocatalytic activity, Ceram. Int. 47 (2021) 10185–10188, https://doi.org/10.1016/j.ceramint.2020.12.070.

[14] M.F. Warsi, B. Bashir, S. Zulfqar, M. Aadil, M.U. Khalid, P.O. Agboola, I. Shakir, M. A. Yousuf, M. Shahid, $Mn_{1-x}Cu_xO_2$/reduced graphene oxide nanocomposites: synthesis, characterization, and evaluation of visible light mediated catalytic studies, Ceram. Int. 47 (2021) 5044–5053, https://doi.org/10.1016/j.ceramint.2020.10.082.

[15] B. Bashir, M.U. Khalid, M. Aadil, S. Zulfqar, M.F. Warsi, P.O. Agboola, I. Shakir, $Cu_xNi_{1-x}O$ nanostructures and their nanocomposites with reduced graphene oxide: synthesis, characterization, and photocatalytic applications, Ceram. Int. 47 (2021) 3603–3613, https://doi.org/10.1016/j.ceramint.2020.09.209.

[16] S. Bashir, A. Habib, A. Jamil, A. Alazmi, M. Shahid, Fabrication of Ag-doped MoO_3 and its nanohybrid with a two-dimensional carbonaceous material to enhance photocatalytic activity, Adv. Powder Technol. 33 (2022), 103482, https://doi.org/10.1016/j.apt.2022.103482.

[17] S. Bashir, A. Jamil, M.S. Khan, A. Alazmi, F.A. Abuilaiwi, M. Shahid, Gd-doped $BiVO_4$ microstructure and its composite with a flat carbonaceous matrix to boost photocatalytic performance, J. Alloys Compd. 913 (2022), 165214, https://doi.org/10.1016/j.jallcom.2022.165214.

[18] M. Aadil, M. Mahmood, M.F. Warsi, I.A. Alsafari, S. Zulfqar, M. Shahid, Fabrication of MnO_2 nanowires and their nanohybrid with flat conductive matrix for the

treatment of industrial effluents, FlatChem 30 (2021), 100316, https://doi.org/10.1016/j.flatc.2021.100316.
[19] M. Fan, B. Hu, X. Yan, C. Song, T. Chen, Y. Feng, W. Shi, Excellent visible-light-driven photocatalytic performance of Cu2O sensitized NaNbO3 heterostructure, New J. Chem. 39 (2015) 6171–6177, https://doi.org/10.1039/C5NJ00751H.
[20] J. Xu, F. Zhang, B. Sun, Y. Du, G. Li, W. Zhang, Enhanced photocatalytic property of Cu doped sodium niobate, Int. J. Photoenergy 2015 (2015), https://doi.org/10.1155/2015/846121. ID 846121.
[21] E.S. Baeissa, Photocatalytic degradation of malachite green dye using Au/NaNbO3 nanoparticles, J. Alloys Compd. 672 (2016) 564–570, https://doi.org/10.1016/j.jallcom.2016.02.024.
[22] M. Sun, Q. Yan, Y. Shao, C. Wang, T. Yan, P. Ji, B. Du, Facile fabrication of BiOI decorated NaNbO3 cubes: a p-n junction photocatalyst with improved visible-light activity, Appl. Surf. Sci. 416 (2017) 288–295, https://doi.org/10.1016/j.apsusc.2017.04.136.
[23] B. Zhang, D. Zhang, Z. Xi, P. Wang, X. Pu, X. Shao, S. Yao, Synthesis of Ag2O/NaNbO3 p-n junction photocatalysts with improved visible light photocatalytic activities, Separ. Purif. Technol. 178 (2017) 130–137, https://doi.org/10.1016/j.seppur.2017.01.031.
[24] Y. Feng, Z. Wang, Y. Yang, X. Wu, X. Gon, Y. Liu, Y. Li, Z. Cao, C. Wang, X. Tong, Chemical bonds-conjugated Ag2SO3/NaNbO3 hybrids as E±cient photocatalysts: in-situ fabrication, characterization and degradation of rhodamine B and methyl orange, Nano 13 (2018), 1850076, https://doi.org/10.1142/S1793292018500765.
[25] Y. Qiao, X. Meng, Z. Zhang, A new insight into the enhanced visible light-induced photocatalytic activity of NaNbO3/Bi2WO6 type-II heterostructure photocatalyst, Appl. Surf. Sci. 470 (2019) 645–657, https://doi.org/10.1016/j.apsusc.2018.11.048.
[26] Y.J. Kim, W. Wu, S.E. Chun, J.F. Whitacre, C.J. Bettinger, Catechol-mediated reversible binding of multivalent cations in eumelanin half-cells, Adv. Mater. 26 (2014) 6572–6579, https://doi.org/10.1002/adma.201402295.
[27] C.T. Chen, F.J. Martin-Martinez, G.S. Jung, M.J. Buehler, Polydopamine and eumelanin molecular structures investigated with ab initio calculations, Chem. Sci. 8 (2017) 1631–1641, https://doi.org/10.1039/C6SC04692D.
[28] W. Xie, E. Pakdel, Y. Liang, D. Liu, L. Sun, X. Wang, Natural melanin/TiO2 hybrids for simultaneous removal of dyes and heavy metal ions under visible light, J. Photochem. Photobiol., A 389 (2020), 112292, https://doi.org/10.1016/j.jphotochem.2019.112292.
[29] Y. Liu, J.D. Simon, Metal-ion interactions and the structural organization of sepia eumelanin, Pigm. Cell Res. 18 (2005) 42–48, https://doi.org/10.1111/j.1600-0749.2004.00197.x.
[30] P. Meredith, K. Tandy, A.B. Mostert, A hybrid ionic–electronic conductor: melanin, the first organic amorphous semiconductor? in: F. Cicoira, C. Santato (Eds.), Organic Eletronics Wiley-VCH Verlag GmbH & Co. KGaA, Weinheim, 2013, pp. 91–111.
[31] P. Kumar, E.D. Mauro, S. Zhang, A. Pezzella, F. Soavi, C. Santato, F. Cicoira, Melanin-based flexible supercapacitors, J. Mater. Chem. C 4 (2016) 9516–9525, https://doi.org/10.1039/C6TC03739A.
[32] L.G.S. Albano, J.V. Paulin, L.D. Trino, S.L. Fernandes, C.F.O. Graeff, Ultraviolet-protective thin film based on PVA–melanin/rod-coated silver nanowires and its application as a transparent capacitor, J. Appl. Polym. Sci. 136 (2019), 47805, https://doi.org/10.1002/app.47805.
[33] Y. Liang, W. Xie, E. Pakdel, M. Zhang, L. Sun, X. Wang, Homogeneous melanin/silica core-shell particles incorporated in poly (methyl methacrylate) for enhanced UV protection, thermal stability, and mechanical properties, Mater. Chem. Phys. 230 (2019) 319–325, https://doi.org/10.1016/j.matchemphys.2019.03.081.
[34] W. Xie, E. Pakdel, Y. Liang, Y.J. Kim, D. Liu, L. Sun, X. Wang, Natural eumelanin and its derivatives as multifunctional materials for bioinspired applications: a review, Biomacrom 20 (2019) 4312–4331, https://doi.org/10.1021/acs.biomac.9b01413.
[35] W. Xie, E. Pakdel, D. Liu, L. Sun, X. Wang, Waste-hair-derived natural melanin/TiO2 hybrids as highly efficient and stable UV-shielding fillers for polyurethane films, ACS Sustainable Chem. Eng. 8 (2020) 1343–1352, https://doi.org/10.1021/acssuschemeng.9b03514.
[36] J.V. Paulin, A.P. Coleone, A. Batagin-Neto, G. Burwell, P. Meredith, C.F.O. Graeff, A.B. Moster, Melanin thin-films: a perspective on optical and electrical properties, J. Mater. Chem. C 9 (2021) 8345–8358, https://doi.org/10.1039/d1tc01440d.
[37] J.V. Paulin, S.L. Fernandes, C.F.O. Graeff, Solid-state electrochemical energy storage based on soluble melanin, Electrochemistry (Tokyo, Jpn.) 2 (2021) 264–273, https://doi.org/10.3390/electrochem2020019.
[38] J. Lu, J. Fang, Ji Li, L. Zhu, Engineering highly transparent UV-shielding flms with disassembled polydopamine oligomers as light adsorber, Appl. Surf. Sci. 550 (2021), 149284, https://doi.org/10.1016/j.apsusc.2021.149284.
[39] X. Zhou, B. Jin, J. Luo, X. Xu, L. Zhang, J. Li, H. Guan, Dramatic visible light photocatalytic degradation due to the synergetic effects of TiO2 and PDA nanospheres, RSC Adv. 6 (2016) 64446–64449, https://doi.org/10.1039/C6RA10292A.
[40] W.-X. Mao, X.-J. Lin, W. Zhang, Z.-X. Chi, R.-W. Lyu, A.-M. Cao, L.-J. Wan, Core-shell structured TiO2@polydopamine for highly active visible-light photocatalysis, Chem. Commun. 52 (2016) 7122–7125, https://doi.org/10.1039/C6CC02041K.
[41] Z. Wang, J. Li, F. Tang, J. Lin, Z. Jin, Polydopamine nanotubes-templated synthesis of TiO2 and its photocatalytic performance under visible light, RSC Adv. 7 (2017) 23535–23542, https://doi.org/10.1039/C7RA03063K.
[42] X. Zhou, B. Jin, J. Luo, X. Gu, S. Zhang, Photoreduction preparation of Cu2O@polydopamine nanospheres with enhanced photocatalytic activity under visible light irradiation, J. Solid State Chem. 254 (2017) 55–61, https://doi.org/10.1016/j.jssc.2017.07.007.
[43] D. Hao, Y. Yang, B. Xu, Z. Cai, Bifunctional fabric with photothermal effect and photocatalysis for highly efficient clean water generation, ACS Sustainable Chem. Eng. 6 (2018) 10789–10797, https://doi.org/10.1021/acssuschemeng.8b02094.
[44] X. Hou, Y. Cai, X. Song, Y. Wu, J. Zhang, Q. Wei, Electrospun TiO2 nanofibers coated with polydopamine for enhanced sunlight-driven photocatalytic degradation of cationic dyes, Surf. Interface Anal. 51 (2019) 169–176, https://doi.org/10.1002/sia.6554.
[45] Y. Zou, Z. Wang, Z. Chen, Q.-P. Zhang, Q. Zhang, Y. Tian, S. Ren, Y. Li, Synthetic melanin hybrid patchy nanoparticle photocatalysts, J. Phys. Chem. C 123 (2019) 5345–5352, https://doi.org/10.1021/acs.jpcc.8b10469.
[46] M. Wang, Z. Cui, M. Yang, L. Lin, X. Chen, M. Wang, J. Han, Core/shell structured CdS/polydopamine/TiO2 ternary hybrids as highly active visible-light photocatalysis, J. Colloid Interface Sci. 544 (2019) 1–7, https://doi.org/10.1016/j.jcis.2019.02.080.
[47] D. Yang, W. Wang, X. Zhao, Z. Zhou, H. Ren, Y. Chen, Z. Zhao, K. An, Z. Jiang, Synthesis of high-efficient g-C3N4/polydopamine/CdS nanophotocatalyst based on bioinspired adhesion and chelation, Mater. Res. Bull. 131 (2020), 110970, https://doi.org/10.1016/j.materresbull.2020.110970.
[48] J. Zhao, J. Chen, Z. Chen, Y. Zhang, D. Xia, Q. Wang, Flexible cotton fabrics/PDA/BiOBr composite photocatalyst using bioinspired polydopamine as electron transfer mediators for dye degradation and Cr(VI) reduction under visible light, Colloids Surf., A 593 (2020), 124623, https://doi.org/10.1016/j.colsurfa.2020.124623.
[49] F. Chena, L. Zhaoa, W. Yua, Y. Wanga, H. Zhanga, L.-H. Guo, Dynamic monitoring and regulation of pentachlorophenol photodegradation process by chemiluminescence and TiO2/PDA, J. Hazard Mater. 399 (2020), 123073, https://doi.org/10.1016/j.jhazmat.2020.123073.
[50] S. Menga, W. Zenga, M. Wanga, L. Niua, S. Hua, B. Sua, Y. Yanga, Z. Yanga, Q. Xue, Nature-mimic fabricated polydopamine/MIL-53(Fe): efficient visible-light responsive photocatalysts for the selective oxidation of alcohols, New J. Chem. 44 (2020) 2102–2110, https://doi.org/10.1039/C9NJ04929K.
[51] L. Carmine, A. Ancona, K. Di Cesare, B. Dumontel, N. Garino, G. Canavese, S. Hernandez, V. Cauda, Sonophotocatalytic degradation mechanisms of Rhodamine B dye via radicals generation by micro- and nano-particles of ZnO, Appl. Catal. B Environ. 243 (2019) 629–640, https://doi.org/10.1016/j.apcatb.2018.10.078.
[52] Q. Jiang, Z. Luo, Y. Men, P. Yang, H. Peng, R. Guo, Y. Tian, Z. Pang, W. Yang, Red blood cell membrane-camouflaged melanin nanoparticles for enhanced photothermal therapy, Biomaterials 143 (2017) 29–45, https://doi.org/10.1016/j.biomaterials.2017.07.02.
[53] V. Capozzi, G. Perna, A. Gallone, P.F. Biagi, P. Carmone, A. Fratello, G. Guida, P. Zanna, R. Cicero, Raman and optical spectroscopy of eumelanin films, J. Mol. Struct. 744 (2005) 717–721, https://doi.org/10.1016/j.molstruc.2004.11.074.
[54] Y. Liu, V.R. Kempf, J.B. Nofsinger, E.E. Weinert, M. Rudnicki, K. Wakamatsu, S. Ito, J.D. Simon, Comparison of the structural and physical properties of human hair eumelanin following enzymatic or acid/base extraction, Pigm. Cell Res. 16 (2003) 355–365, https://doi.org/10.1034/j.1600-0749.2003.00059.x.
[55] Y. Liu, L. Hong, K. Wakamatsu, S. Ito, B. Adhyaru, C.-Y. Cheng, C.R. Bowers, J. D. Simon, Comparison of structural and chemical properties of black and red human hair melanosomes, Photochem. Photobiol. 81 (2005) 135–144, https://doi.org/10.1562/2004-08-03-RA-259.1.
[56] V. Capozzi, G. Perna, P. Carmone, A. Gallone, M. Lastella, E. Mezzenga, G. Quartucci, M. Ambrico, V. Augelli, P.F. Biagi, T. Ligonzo, A. Minafra, L. Schiavulli, M. Pallara, R. Cicero, Optical and photoelectronic properties of melanin, Thin Solid Films 511 (2006) 362–366, https://doi.org/10.1016/j.tsf.2005.12.065.
[57] P. Meredith, B.J. Powell, J. Riesz, S.P. N.R, M.R. Pedersonc, E.G. Moore, Towards structure–property–function relationships for eumelanin, Soft Matter 2 (2006) 37–44, https://doi.org/10.1039/b511922g.
[58] D.L. Wood, J. Tauc, Weak absorption tails in amorphous semiconductors, Phys. Ver. B. 5 (1972) 3144–3151, https://doi.org/10.1103/PhysRevB.5.3144.
[59] D. Niyonkuru, A. Carrière, R. Ambrose, A. Gouda, M. Reali, A. Camus, A. Pezzella, I. Hillb, C. Santato, Locating the bandgap edges of eumelanin thin films for applications in organic electronic, J. Chem. Technol. Biotechnol. 97 (2022) 837–843.
[60] W. Xu, W. Yang, H. Guo, L. Ge, J. Tu, C. Zhen, Constructing a TiO2/PDA core/shell nanorod array electrode as a highly sensitive and stable photoelectrochemical glucose biosensor, RSC Adv. 10 (2020) 10017–10022, https://doi.org/10.1039/C9RA10445C.